

Thermal Modelling for Preventing Eye Injuries in Workplaces with High Environmental Temperatures

Original

Thermal Modelling for Preventing Eye Injuries in Workplaces with High Environmental Temperatures / Grisolia, G.; Lucia, U.. - In: APPLIED SCIENCES. - ISSN 2076-3417. - STAMPA. - 16:(2026), pp. 1-13. [10.3390/app16073531]

Availability:

This version is available at: 11583/3009602 since: 2026-04-03T15:53:07Z

Publisher:

MDPI

Published

DOI:10.3390/app16073531

Terms of use:



This article is made available under terms and conditions as specified in the corresponding bibliographic description in the repository

Publisher copyright

(Article begins on next page)

Article

Thermal Modelling for Preventing Eye Injuries in Workplaces with High Environmental Temperatures

Giulia Grisolia ^{1,*}  and Umberto Lucia ^{2,*} 

¹ Dipartimento di Ingegneria dell’Ambiente, del Territorio e delle Infrastrutture, Politecnico di Torino, Corso Duca degli Abruzzi 24, 10129 Torino, Italy

² Dipartimento Energia “Galileo Ferraris”, Politecnico di Torino, Corso Duca degli Abruzzi 24, 10129 Torino, Italy

* Correspondence: giulia.grisolia@polito.it (G.G.); umberto.lucia@polito.it (U.L.); Tel.: +39-011-090-4558 (U.L.)

Abstract

Elevated temperatures are frequently encountered in numerous occupational settings such as iron and steel foundries, non-ferrous metal foundries, brick and ceramic manufacturing plants, glass production facilities, rubber factories, electrical power plants, bakeries, laundries, chemical processing sites, mining operations, smelting plants, and steam tunnels. Employees working in these environments are at risk of developing various health issues and injuries, including ocular complications, due to prolonged exposure to heat and the physical demands of handling heavy materials. This study focuses on examining the pressure within the eye’s anterior chamber, referred to as Intraocular Pressure (IOP), and its association with the cornea’s biomechanical characteristics, with particular attention to corneal temperature. Our methodology is grounded in the principles of the first law of thermodynamics. The findings reveal a link between the temperature of the eye’s anterior chamber and the biomechanical behaviour of the cornea. Specifically, IOP serves as an indicator of the cornea’s elasticity and its optical properties as influenced by temperature variations. We investigated how the cornea’s elastic energy, or the work it performs, varies with temperature changes. The results show that an increase in temperature corresponds to a reduction in the work exerted by the cornea. The corneal temperature is affected by both the ambient environment and the temperature of the aqueous humour within the anterior chamber. This indicates a relationship between the mechanical work done by the cornea and the pressure exerted by the fluid in the eye’s front segment. Furthermore, our study identified a correlation between corneal thickness and IOP, which our modelling approach successfully quantifies. Utilizing the first law of thermodynamics, we calculated the work performed by the anterior chamber against the cornea’s internal surface. Temperature fluctuations influence the secretion, drainage, and flow characteristics of the aqueous humour, thereby impacting IOP and associated ocular conditions. These insights are valuable for devising strategies aimed at preventing eye injuries among workers exposed to high-temperature environments.



Academic Editor: Piotr Gas

Received: 5 March 2026

Revised: 28 March 2026

Accepted: 3 April 2026

Published: 3 April 2026

Copyright: © 2026 by the authors.

Licensee MDPI, Basel, Switzerland.

This article is an open access article distributed under the terms and conditions of the [Creative Commons Attribution \(CC BY\) license](https://creativecommons.org/licenses/by/4.0/).

Keywords: bio-engineering thermodynamics modelling; thermo-elasticity of ocular tissues; cornea; intraocular pressure; glaucoma risk; occupational health and eye injury prevention

1. Introduction

The workplace can be a dynamic environment filled with various tasks and machinery that pose potential risks to our eyes. Common types of eye hazards include chemical, mechanical, biological, and radiation risks, all of which can lead to thermal stress or injury.

Eye injuries can result in severe and long-lasting consequences, such as vision loss, blindness, pain, discomfort, corneal abrasions, chemical burns, conjunctivitis, detached retinas, cataracts, glaucoma, and secondary infections. It is crucial to recognise the potential outcomes of eye injuries and take proactive measures to prevent them. Using proper eye protection, adhering to safe work practices, and seeking immediate medical attention in the event of an injury can significantly reduce the risk of these adverse effects.

Numerous workplaces such as iron and steel foundries, non-ferrous metal foundries, brick and ceramic manufacturing plants, glass factories, rubber production sites, electrical utilities, bakeries, laundries, chemical processing facilities, mining operations, smelting plants, and steam tunnels are included, frequently subject workers to elevated temperatures. Employees in these industries may experience various diseases and injuries, including eye problems, due to extreme heat and the handling of heavy materials.

Such injuries not only impact the individuals affected but also compromise workplace productivity and safety. We often take our vision for granted in our daily routines, making the importance of eye safety tips in the workplace even more evident.

This study seeks to examine the pressure in the anterior chamber of the eye, referred to as intraocular pressure (IOP), and its relationship with the biomechanical properties of the cornea, particularly regarding its temperature. Our approach is founded on the first law of thermodynamics [1]. Our objective is to establish a link between the temperature within the eye's anterior chamber and the cornea's biomechanical properties. Intraocular Pressure (IOP) serves as a measure of the cornea's elasticity and its refractive behaviour as influenced by temperature changes. We investigate how the cornea's elastic energy, or potential work, varies with temperature fluctuations. The findings indicate that an increase in temperature leads to a reduction in the work performed by the cornea. The temperature of the cornea is influenced both by the external environment and the temperature of the fluid present in the eye's anterior segment. This suggests a connection between the mechanical work exerted by the cornea and the pressure exerted by the fluid in the anterior chamber.

Additionally, our study reveals a relationship between corneal thickness and IOP, which our modelling methods effectively elucidate. To achieve this, we apply the first law of thermodynamics to quantify the work done by the anterior chamber against the cornea's inner surface. Temperature variations impact the secretion, drainage, and flow characteristics of the aqueous humour, thereby influencing intraocular pressure and related ocular conditions. This understanding is crucial for creating preventive measures to safeguard workers' eyes from injuries, particularly concerning glaucoma and keratoconus caused by mechanical trauma. Glaucoma is a condition that results in progressive vision loss due to IOP abnormalities and is a leading cause of blindness. Accurate IOP assessment is vital after surgeries related to corneal, lenticular, and vitreoretinal issues. Central corneal thickness (CCT) significantly impacts tonometry, and measuring CCT using pachymetry has become routine for precise IOP evaluation. Nonetheless, different algorithms for IOP correction yield varying outcomes, underscoring the necessity for a standardised analysis approach.

The biomechanical properties of the cornea are complex, characterized by [2–12]:

- Heterogeneity, in dimensional properties;
- Near incompressibility, due to water and collagen fibres (Poisson's ratio ~ 0.5);
- Nonlinear responses when intraocular pressure varies;
- Demonstrating viscoelastic and creep characteristics during testing;
- Showing structural anisotropy due to the alignment of collagen fibrils.

Biomechanical factors [2–4] play a significant role in conditions such as keratoconus, characterised by a decrease in corneal stiffness, and corneal ectasia following refractive surgery, which leads to deformation. Recent research indicates that measuring corneal temperature is essential for diagnosing eye diseases. Although several models exist for

examining corneal characteristics and heat exchange, there is currently no all-encompassing model that connects these characteristics with the thermal dynamics of the anterior chamber. This relationship is crucial for understanding the flow of aqueous humour, which regulates IOP and contributes to visual stability. Temperature influences tissue metabolism; however, there is a lack of theoretical models that facilitate clinical assessment. Given these intricacies, we suggest a novel approach utilising irreversible bioengineering thermodynamics to explore the interplay between IOP and corneal properties, with a particular focus on the glaucoma risk in patients with hypertension.

2. Materials and Methods

To apply a thermodynamic perspective to assessing the risk of eye injuries in occupational settings, we treated the intraocular-pressure-related flows as water moving in and out between the eye's anterior chamber and the surrounding blood vessels.

Intraocular pressure (IOP) is dynamically modulated by the contractile behaviour and viscoelastic properties of the trabecular meshwork (TM). Contemporary models of aqueous humour outflow have moved beyond viewing the TM as a passive structure merely stretched by the ciliary muscle (CM). Instead, substantial evidence now indicates that the trabecular meshwork exhibits smooth muscle-like characteristics, actively participating in the regulation of aqueous humour drainage and IOP control [13]. Recent investigations have identified the polymodal cation channel TRPV4 as a key mechanosensor within this system, integrating mechanical, biochemical, and circadian inputs to finely tune IOP levels [14]. Within this framework, the TM and CM function as physiological antagonists: contraction of the ciliary muscle causes distension of the trabecular meshwork, thereby reducing aqueous outflow, whereas contraction of the trabecular meshwork itself promotes increased outflow. The signalling pathways governing relaxation and contraction in both the ciliary muscle and trabecular meshwork can be categorised based on their dependence on membrane voltage changes and extracellular calcium influx, with additional pathways likely yet to be elucidated. These pathways involve distinct ion channels and exhibit differential expression patterns in the TM and CM, resulting in varied responses to pharmacological agents that induce relaxation or contraction [13]. Furthermore, ambient temperature appears to influence IOP through complex nonlinear mechanisms and cumulative short-term effects, particularly in individuals without glaucoma, underscoring the importance of environmental temperature monitoring in IOP management [15]. Elevated temperatures can induce collagen shrinkage, potentially affecting the tension-sensitive lamellae of the trabecular meshwork or the ciliary muscle itself [16].

In order to develop the study of the outside temperature effect on the eye, we consider it as an open system, because it can exchange water and heat. To do so, we must define the border of the system. We consider the full eyeball (in geometrical approximation, an ellipsoid) as the border. In this way, the thermodynamic approach allows us to consider heat and work exchanged only at the boundary. In particular, the cornea is exposed to the environment, and it is affected by heat flow, while the rest of the eye is inside the human body, and we can consider it at the same temperature as the body itself [17]. In this thermodynamic framework, work is related to the external forces, allowing us to not consider the intraocular biomechanical interactions [7,18]. Therefore, by viewing the eye as an open system in relation to the body, we utilize the first law of thermodynamics [1]:

$$\dot{Q} - \dot{W} = \frac{d}{dt} \left[U + p_0 V + \int_v \rho(e_k + e_p) dV \right]_{CV} + \dot{m}_{out} (h + e_k + e_p)_{out} + \dot{m}_{in} (h + e_k + e_p)_{in} \quad (1)$$

where \dot{Q} [W] is the heat power exchanged between the cornea and the external environment, \dot{W} [W] is the mechanical power carried out by the tissue concerning the pressure and elastic

properties of the cornea, U [W] is the internal energy, p_0 [Pa] is the external environmental pressure, V is the volume of the anterior chamber, ρ [kg m^{-3}] is the water density, e [J kg^{-1}] is the specific energy, k stands for kinetic, p [Pa] as a subscript means potential, h is the specific enthalpy of the water, \dot{m} [kg s^{-1}] is the mass flow, in means inflow, out means outflow, and CV means control volume.

The water inflow temperature T_{in} is usually assumed equal to the artery temperature of 36.7°C [19] while the water outflow temperature T_{out} is assumed the eye's anterior chamber temperature of $(30.7 \pm 1.7)^\circ\text{C}$ [20]. In stationary and healthy conditions, water volume flows results $\dot{V}_{in} = \dot{V}_{out} = (2.25 \pm 0.75) \mu\text{L min}^{-1}$ [21]. Water density obtained by interpolation of the values in the range $t \in [25.0, 40.0]^\circ\text{C}$ [22]:

- in relation to water
 - inflow water at 36.7°C : 993 kg m^{-3} , that brings to a mass inflow of $(3.73 \pm 1.24) \times 10^{-8} \text{ kg s}^{-1}$
 - outflow water at 30.7°C : 996 kg m^{-3} , that brings to a mass outflow of $(3.73 \pm 1.24) \times 10^{-8} \text{ kg s}^{-1}$
- Water specific enthalpy evaluated by using the following equation [22]

$$h(T) = h_{sat}(T) + v_{sat}(T) \cdot (p - p_{sat}(T)) \quad (2)$$

where $h_{sat}(T)$ is the water saturation enthalpy at the temperature T , $p_{sat}(T)$ is the water saturation pressure at the temperature T , $v_{sat}(T)$ is the water saturation specific volume at the temperature T and p is the working pressure. and the table of water properties in Ref. [22]:

- inflow: value at inflow mean pressure (93 mmHg) of $h_{av,in} = 153.75 \text{ kJ kg}^{-1}$;
- outflow: value at inflow mean pressure (93 mmHg) and in the temperature range $(30.7 \pm 1.7)^\circ\text{C}$, with $h_{av,out} = 128.67 \text{ kJ kg}^{-1}$ at its central value;
- Water enthalpy rate evaluated as $\dot{H} = dH/dt = \dot{m} h_{av}$ Ref. [22]:
 - inflow: $\dot{H} = \dot{m}_{in} h_{av,in} = (5.73 \pm 1.91) \text{ mW}$;
 - outflow: $\dot{H} = \dot{m}_{out} h_{av,out} = (4.81 \pm 1.60) \text{ mW}$.

The kinetic and potential energies are negligible and can be treated as zero. Indeed, the aqueous humour in the eye's anterior chamber is produced behind the iris and flows into the anterior chamber through the pupil, while it exits primarily via specialised outflow structures located at the iridocorneal angle. Aqueous humour production exhibits a diurnal variation, averaging around $2.3 \mu\text{L min}^{-1}$. Specifically, production rates were recorded as $2.91 \pm 0.71 \mu\text{L min}^{-1}$ between 08:00 and 12:00, $2.66 \pm 0.58 \mu\text{L min}^{-1}$ between 12:00 and 16:00, and $1.23 \pm 0.41 \mu\text{L min}^{-1}$ between 00:00 and 06:00 [23]. Using a representative production rate of $2.25 \mu\text{L min}^{-1}$ (approximately $4.2 \times 10^{-11} \text{ m}^3 \text{ s}^{-1}$) and assuming a minimum pupil aperture radius of 1 mm, the corresponding average flow velocity through the pupil is estimated at $1.3 \times 10^{-5} \text{ m s}^{-1}$. This relatively low velocity suggests that, except under extreme conditions, the flow through the pupil aperture does not substantially affect the overall fluid dynamics within the anterior chamber [23]. The primary aqueous humour outflow occurs through the trabecular meshwork (TM) and Schlemm's canal (SC), which together form a continuous 360-degree filtration system. The relevant anatomical features and their dimensions, which influence flow velocities and resistance, include:

- Schlemm's Canal Area: The canal's cross-sectional area ranges from approximately 4064 to $7164 \mu\text{m}^2$. Its lumen is elliptical, with a radial depth between 190 and $370 \mu\text{m}$ and a total circumference near 36 – 40 mm , providing a significant conduit for aqueous outflow;

- Trabecular Meshwork (TM) Area: The TM has a triangular cross-section with a base width of 50–150 μm and a meridional length (along the cornea) ranging from about 350 μm to over 500 μm, depending on age and location. These dimensions critically affect the velocity and resistance of fluid passing through this tissue;
- Collector Channel Ostia: Aqueous humour exits Schlemm’s canal via 25–35 collector channels, whose openings vary in diameter from 5 to 50 μm, occasionally reaching up to 70 μm. The size and number of these ostia influence the velocity of fluid leaving the canal;
- Juxtacanalicular Tissue (JCT): This thin layer, approximately 2–20 μm thick, situated between the trabecular meshwork and Schlemm’s canal, represents the most significant resistance point in the outflow pathway, thereby strongly impacting local flow velocities.

Together, these anatomical features govern the velocity profiles and resistance encountered by aqueous humour as it flows through the anterior chamber and exits the eye, playing a crucial role in maintaining intraocular pressure homeostasis. As a consequence of these anatomic values, the kinetic energy contribution to the first law results in the order of 10^{-15} mW, negligible in relation to the enthalpy contribution. Thus, the eye’s behaviour over the observation period allows us to perform a time integration, obtaining:

$$Q - W = (m_{out} - m_{in}) c_w T_w + p_0 \Delta V + m_{out} c_p T_w - m_{in} c_p T_{in} \tag{3}$$

In this context, $c_w = 4186 \text{ J kg}^{-1} \text{ K}^{-1}$ represents the specific heat capacity of the water inside the anterior chamber at constant volume, while $c_p [\text{J kg}^{-1} \text{ K}^{-1}]$ denotes the specific heat capacity at constant pressure. The temperature within the anterior chamber is T_w , and the inflowing water temperature is $T_{in} = 37 \text{ }^\circ\text{C}$. The mass of the water is $m_w [\text{kg}]$, and the external environmental temperature, T_0 , varies within the range of $-30 \text{ }^\circ\text{C}$ to $+30 \text{ }^\circ\text{C}$. The term $\Delta V [\text{m}^3]$ corresponds to the change in volume caused by water stagnation inside the ocular anterior chamber. Assuming that the anterior chamber exchanges heat with the surrounding environment through the corneal surface, the first law of thermodynamics can be applied to this system considering that $Q [\text{J}]$ is the result of the heat fluxes and can be evaluated as the rate of internal energy variation:

$$Q = \int_0^t \left(\frac{T_c - T_{out}}{R_{cd}} + \frac{T_0 - T_c}{R_{cv}} + \sigma (T_0^4 - \epsilon T_c^4) A \right) dt + m_t r = -m_w c_v (T_w - T_0) \tag{4}$$

where R_{cd} and $R_{cv} = 1/(\alpha A)$ are the conductive and convective resistance respectively [22], $\sigma = 5.67 \times 10^{-8} \text{ W m}^{-2} \text{ K}^{-4}$ is the Stefan-Boltzmann constant [22], $A = (1.3 - 1.4) \text{ cm}^2$ is the area of the surface of the cornea and d is its thickness, m_t is the evaporated tear mass and r is its latent heat of evaporation. The conductive heat power must be considered in relation to the cornea’s geometry.

Consequently, we can obtain:

$$-W = (m_{out} - m_{in}) c_w T_w + p_0 \Delta V - m_{in} c_p T_{in} + m_w c_v (T_w - T_0) \tag{5}$$

Then, we can evaluate the work carried out by the water against the external surface of the anterior chamber as:

$$W = -V \Delta \text{IOP} \tag{6}$$

where we consider that for each $10 \text{ }^\circ\text{C}$ decrease in air temperature corresponds an increase in IOP of roughly 0.2 to 0.3 mmHg [24], and the ocular anterior chamber temperature results in:

$$T_w = \frac{V \Delta \text{IOP} - \text{IOP} \Delta V}{c_w (2m_{out} - m_{in} + m_w)} + \frac{m_{in} T_{in} + m_w T_0}{2m_{out} - m_{in} + m_w} \tag{7}$$

where

$$\Delta V = \beta V \Delta T \tag{8}$$

with $\beta \approx 2.1 \times 10^{-4} \text{ K}^{-1}$ for water at human body temperature. Let $c_w = c_p = c_v$ represent the specific heat capacity of liquid water. In a healthy eye without pressure-related issues, the mass flow rate exiting the anterior chamber, m_{out} , is approximately equal to the mass flow rate entering it, m_{in} . The external pressure p_0 is set at 101,325 Pa, while the intraocular pressure, typically around $16 \pm 2 \text{ mmHg}$ [25], corresponds to the pressure exerted by the anterior chamber against the elastic resistance of the cornea’s posterior wall. Based on this framework, heat exchange within the anterior chamber is assumed to occur via the corneal surface. The main mechanisms of heat transfer include conduction across the cornea’s thickness and convection between the cornea’s outer surface and the ambient air. Therefore, the corneal temperature T_c can be determined using the standard heat transfer methodology as described in reference [26], expressed as follows:

$$T_c = T_w + \frac{T_w - T_0}{\frac{s}{\lambda} + \frac{1}{\alpha}} \tag{9}$$

In the context of references [26–29], s represents the average thickness of the cornea, approximately 0.5 mm, λ denotes the thermal conductivity of the cornea, valued at $0.6 \text{ W m}^{-1} \text{ K}^{-1}$ and α is the convective heat transfer coefficient, taken as $50 \text{ W m}^{-2} \text{ K}^{-1}$. The results derived from this analysis are illustrated in Figure 1. It is important to highlight that the corneal temperature is predominantly influenced by environmental temperature and plays a significant role in the fluctuations of the anterior chamber temperature. The data obtained align closely with previously published findings in the literature [26–39], as reviewed in the earlier section, with discrepancies below 1% (see also Refs. [27,29]). The observation period considered in this study exceeds the thermal transient duration, which has been estimated to be around 5000 s [27].

Now, considering the extended Bernoulli’s equation:

$$W = \int_V p dV - p_0 \Delta V - W_\lambda - \Delta E_k - \Delta E_p \tag{10}$$

where W_λ is the work lost for irreversibility, E_k is the kinetic energy and E_p is the cornea elastic potential energy, and introducing this into Relation (5) it follows that the elastic potential variation of the cornea results as:

$$\Delta E_p = (m_{out} - m_{in}) c_w T_w + m_{out} c_w T_w - m_{in} c_w T_{in} + m_w c_w (T_w - T_0) \tag{11}$$

This outcome is illustrated in Figure 2. The shape was derived under the assumption that both kinetic energy and work lost due to irreversibility are negligible. It is important to highlight that the elastic work of the cornea (i.e., the change in elastic potential energy) is influenced by the cornea’s temperature.

Finally, considering Relations (7) and (11), it follows that:

$$\Delta E_p = Y s = (2 m_{out} - m_{in}) c_w \left[\frac{V \Delta IOP}{c_w (2 m_{out} - m_{in} + m_w)} + \frac{m_{in} T_{in} + m_w T_0}{2 m_{out} - m_{in} + m_w} \right] - m_{in} c_w T_{in} + m_w c_w \left[\frac{V \Delta IOP}{c_w (2 m_{out} - m_{in} + m_w)} + \frac{m_{in} T_{in} + m_w T_0}{2 m_{out} - m_{in} + m_w} - T_0 \right] \tag{12}$$

where Y is the Young modulus and s is the cornea thickness.

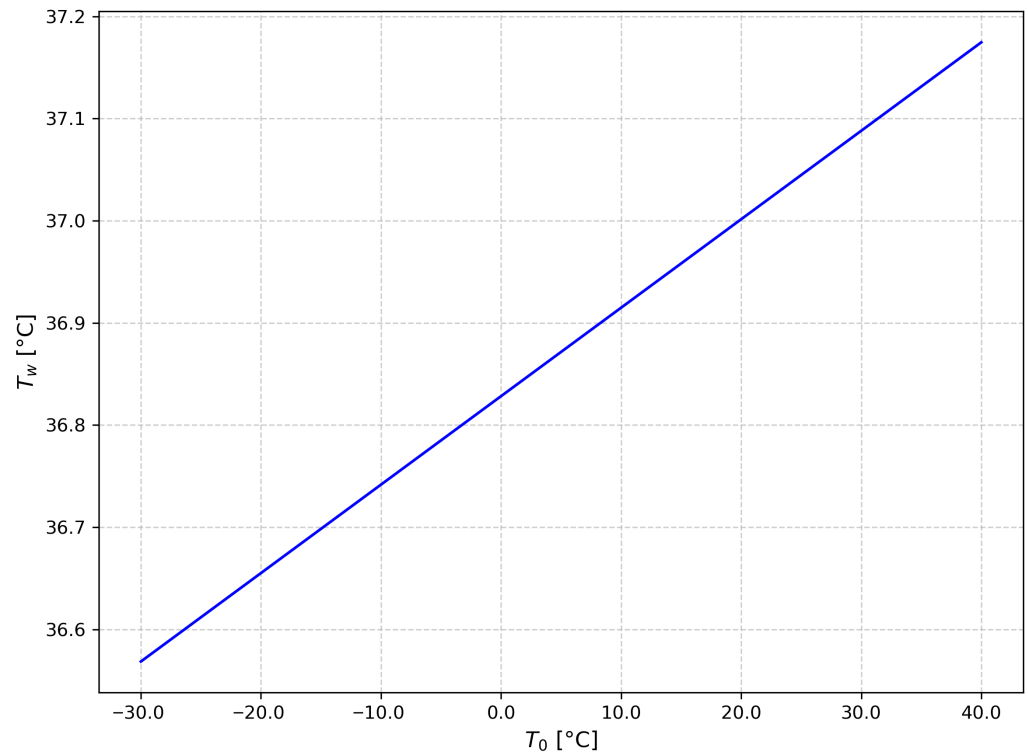


Figure 1. Temperature of the ocular anterior chamber (T_w) evaluated by using Equation (6) in relation to the variation of external environmental temperature (T_0).

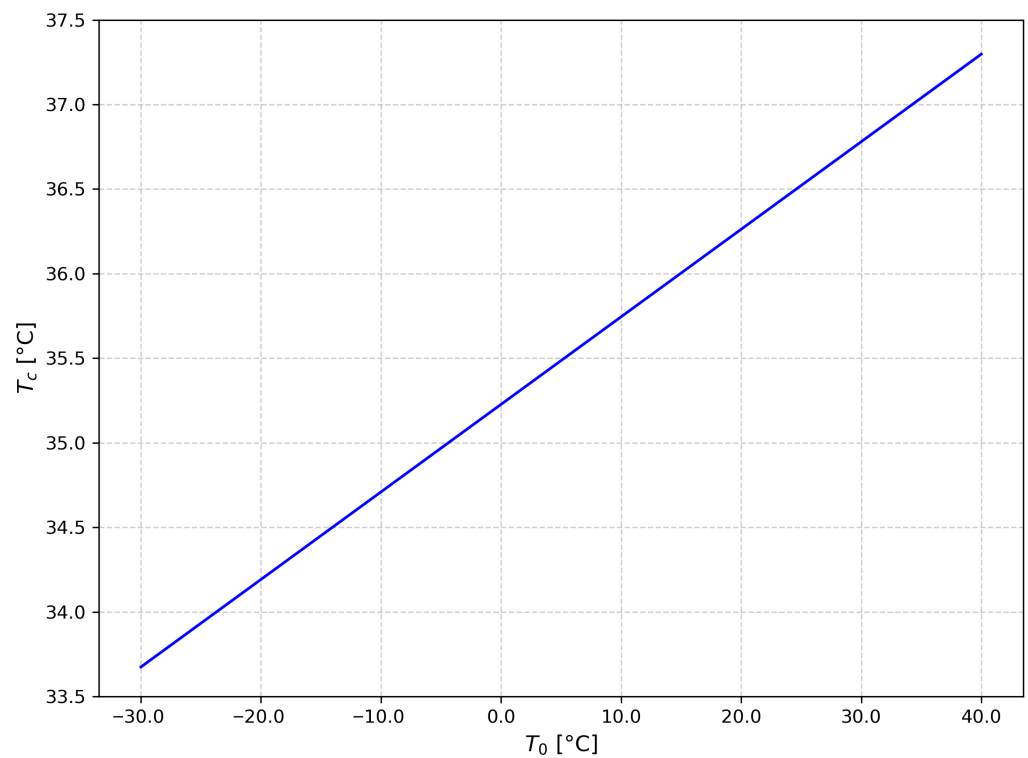


Figure 2. Temperature of the ocular cornea (T_c) evaluated by using Equation (7) in relation to the variation of external environmental temperature (T_0).

3. Results

The thermodynamic approach enables us to effectively analyse how liquid flow affects the anterior chamber of the eye. Our findings establish a clear connection between the temperature within the anterior chamber and the surrounding environmental temperature.

As shown in Figure 1, the temperature of water in the anterior chamber, while in Figure 2, the temperature of the cornea consistently rises in response to increasing environmental temperatures. This observation highlights the importance of environmental factors in affecting ocular temperatures.

Figure 3 illustrates the cornea's elastic potential energy in relation to its temperature, showing a clear decline in elastic potential energy as corneal temperature increases. Our results are consistent with earlier studies referenced in [15,17], as well as recent research on humans [37–39]. These investigations confirm that eyes with ischemic central venous retinal occlusion, which results from elevated pressure, have lower ocular surface temperatures compared to non-ischemic eyes. This correlation supports our findings, indicating that corneal potential energy is directly related to intraocular pressure.

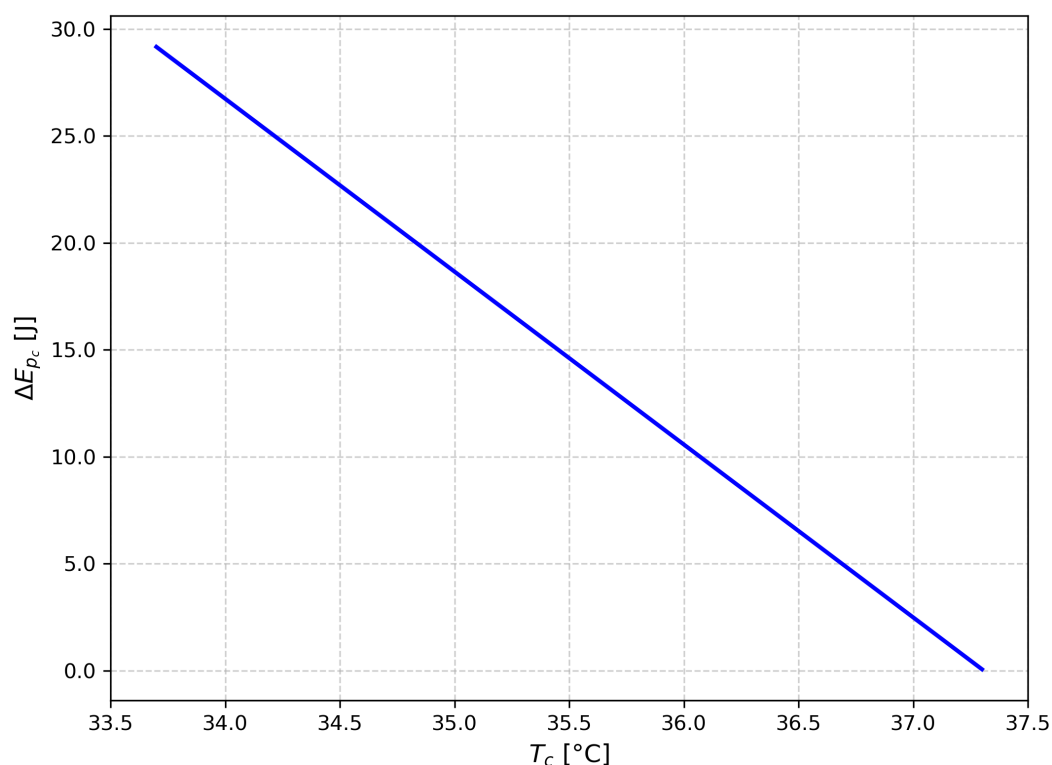


Figure 3. Elastic properties of the cornea as a function of cornea temperature, evaluated by using Equation (12).

As a result, lower temperatures result in higher potential energy in the cornea and an increase in intraocular pressure, leading to significant ischemic effects on the optic nerve. Our findings align with the experimental data presented in previous studies (Refs. [26–29,31]). It is important to emphasise that corneal temperature is primarily affected by the environmental temperature, rather than that of the anterior chamber.

In assessing the elastic work (the change in potential energy) of the cornea in relation to corneal temperature, we observed a noticeable reduction in work as temperature increases. It is worth noting that corneal temperature is influenced by both environmental and anterior chamber temperatures. Thus, there is an analytical link between the elastic work done by the cornea in relation to anterior chamber pressure and temperature, as well as between corneal thickness and intraocular pressure (IOP).

Our analysis provides insight into this relationship. Based on Equation (12), it is evident that the variation between the fluid inflow and outflow plays a crucial role in influencing the cornea's elastic characteristics and the resulting intraocular pressure (IOP).

In Figure 4, the risk condition is identified: this occurs when the temperature of the cornea exceeds that of the anterior chamber, indicating that the eye cannot dissipate heat, leading to a rise in temperature and an associated increase in pressure, which may harm the optic nerve.

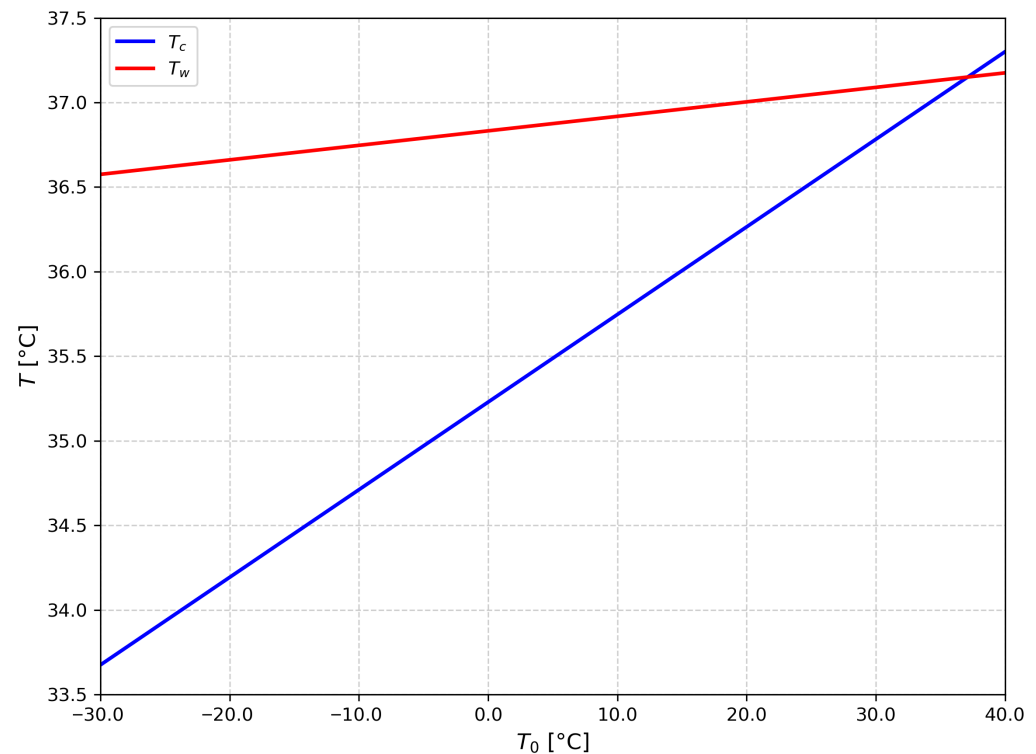


Figure 4. Risk condition. Thermal risk thresholds are determined through the intersection of water and corneal temperature as shown in the graphics.

These findings highlight that:

- Any mechanical stress leads to a change in temperature, resulting in a variation in intraocular pressure (IOP);
- Any temperature change is linked to a rise in IOP, which elevates the risk of developing glaucoma.

As a result, it may be beneficial to utilise glasses equipped with an electronic thermometer to monitor the temperature exposure of workers' eyes. Indeed, in recent years, smart glasses have garnered significant interest due to their convenient capabilities, including hands-free augmented reality experiences. However, because these devices are worn in direct contact with the face and head, elevated device temperatures can adversely impact users' physical health [40]. The study and analysis of smart devices fall outside the scope of this paper; however, they represent a promising area for future research.

4. Discussion and Conclusions

Glaucoma is a significant optic neuropathy characterised by the degeneration of ganglion cells and their fibers, which can lead to irreversible visual field loss and, in severe cases, blindness. Maintaining intraocular pressure (IOP) is critical for preventing further damage from glaucoma and preserving vision. Elevated IOP is clearly a major risk factor for

the development of this disease. Thermography has proven to be effective in investigating the vascular aspects related to the pathology of glaucoma, indicating that ocular surface temperature can serve as a reliable measure of compromised retrobulbar hemodynamics in glaucoma studies [29,37].

The cornea is the eye's main refractive component, composed of five individual layers: the epithelium, Bowman's layer, stroma, Descemet's membrane, and endothelium. Its dimensions typically include a radius of 10–11 mm and a thickness of approximately 0.5 mm.

The cornea plays a crucial role in regulating heat exchange with its surroundings and the anterior chamber, making its surface temperature vital for maintaining a stable temperature within the anterior chamber. Precise determination of corneal temperature can be accomplished by analysing the conductive heat transfer occurring through the cornea, thereby directly correlating the corneal temperature with that of the anterior chamber. Moreover, the cornea's elastic properties play a vital role in affecting intraocular pressure (IOP) measurements. According to the hypothesis proposed by Goldmann and Schmidt in 1957, IOP readings tend to be underestimated in individuals with thinner corneas and overestimated in those with thicker corneas [32,41,42]. This theory has been experimentally supported [38], confirming a consistent relationship between corneal thickness and IOP, which is influenced by two primary factors:

- Swelling Pressure (SP): The force generated by the repulsion of negatively charged glycosaminoglycans within the corneal stroma;
- Imbibition Pressure (IP): The negative pressure that drives fluid absorption into the cornea. Therefore, the intraocular pressure (IOP) can be expressed as the sum of these two components: $IOP = SP + IP$.

Based on our findings, we can draw the following conclusions:

- A correlation exists between the temperature of the ocular anterior chamber and intraocular pressure (IOP);
- The temperature of the cornea is linked to the temperature within the ocular anterior chamber;
- The elastic properties of the cornea are influenced by its temperature;
- There is an association between IOP and corneal thickness, which can be assessed through measurements of the ocular anterior chamber temperature.

The first law of thermodynamics can be applied to evaluate the work done by the anterior chamber against the cornea's internal surface. The temperature of the aqueous humour is influenced by the balance between heat lost through the cornea and heat generated by metabolic activity and blood flow within the anterior chamber. Consequently, temperature plays a crucial role in controlling the secretion, drainage, and circulation of aqueous humour, which in turn affects the regulation of intraocular pressure and conditions such as glaucoma.

Moreover, the relationship between the temperatures of the anterior chamber and cornea can provide insights into tear film evaporation and its connection to environmental factors. It is also possible that different isotopes of transient receptor potential channels may significantly influence aqueous humour dynamics, as indicated by Fabiani [29]. Thus, temperature could emerge as a novel target for managing the progression of glaucoma in patients with ocular hypertension. It is particularly noteworthy that ocular temperature tends to decrease with age, making it essential to assess each patient's individual evolution in this context.

Additionally, a strong connection has been experimentally established between corneal elastic properties, refractive errors, and characteristics of the anterior chamber, validating

our theoretical insights. Recent research indicates that eyes affected by ischaemic central venous retinal occlusion (CRVO) exhibit lower ocular surface temperatures compared to non-ischaemic eyes. Additionally, studies by Galassi et al. [37] have identified ocular surface temperature as a useful marker for detecting impaired retrobulbar haemodynamics in patients with glaucoma. This suggests that ocular surface temperature measurements can provide valuable insights into vascular and haemodynamic changes associated with these ocular conditions.

By using a thermodynamic approach, we can evaluate liquid flows within the ocular anterior chamber. Fluctuations in mass flow within this chamber can result in variations in intraocular pressure (IOP), which subsequently influence the cornea's elastic properties. These corneal characteristics, in turn, have an impact on the refractive properties of the eye; therefore, changes in IOP can also be reflected in alterations in vision. IOP is primarily dependent on the dynamics of aqueous humour, which is regulated through a balance of secretion and excretion. Aqueous humour formation occurs via three mechanisms: diffusion, ultrafiltration, and active secretion.

In summary, in accordance with the experimental results obtained by Fabiani et al. [29] and by Yoshida et al. [15], there is a notable correlation between IOP and temperature, which can be gauged using non-contact measurement systems. This feature is crucial for the development of non-contact tonometers aimed at future home monitoring and personalised therapy. Finally, the findings underscore the potential risks in certain work environments and highlight temperature as a critical risk factor, pointing to the need for innovative devices that can measure proximal eye temperature. The risk temperature results are ≥ 38 °C with an error of 1% evaluated by the standard deviation. Our result is comparable with the result in literature ($\simeq 40$ °C) [43].

Author Contributions: Conceptualization, U.L. and G.G.; methodology, U.L. and G.G.; software, G.G.; validation, U.L. and G.G.; formal analysis, U.L.; investigation, U.L. and G.G.; resources, U.L.; data curation, G.G.; writing—original draft preparation, U.L. and G.G.; writing—review and editing, U.L. and G.G.; visualization, G.G.; supervision, U.L.; project administration, U.L.; funding acquisition, U.L. All authors have read and agreed to the published version of the manuscript.

Funding: This research received no external funding.

Institutional Review Board Statement: Not applicable.

Informed Consent Statement: Not applicable.

Data Availability Statement: The original contributions presented in this study are included in the article. Further inquiries can be directed to the corresponding authors.

Conflicts of Interest: The authors declare no conflicts of interest.

References

1. Lucia, U.; Grisolia, G. Thermal Physics and Glaucoma: From Thermodynamic to Biophysical Considerations to Designing Future Therapies. *Appl. Sci.* **2020**, *10*, 7071. <https://doi.org/10.3390/app10207071>.
2. Lucia, U.; Grisolia, G. Thermal Resonance and Cell Behavior. *Entropy* **2020**, *22*, 774. <https://doi.org/10.3390/e22070774>.
3. Lucia, U.; Grisolia, G. From Ion Fluxes in Living Cells to Metabolic Power Considerations. *Mathematics* **2023**, *11*, 2645. <https://doi.org/10.3390/math11122645>.
4. Lucia, U. Bioengineering thermodynamics: An engineering science for thermodynamics of biosystems. *Int. J. Thermodyn.* **2015**, *18*, 254–265. <https://doi.org/10.5541/ijot.5000131605>.
5. Ehlers, N.; Hansen, F.K.; Aasved, H. Biometric Correlations of Corneal Thickness. *Acta Ophthalmol.* **1975**, *53*, 652–659. <https://doi.org/10.1111/j.1755-3768.1975.tb01784.x>.
6. Johnson, M.; Kass, M.A.; Moses, R.A.; Grodzki, W.J. Increased Corneal Thickness Simulating Elevated Intraocular Pressure. *Arch. Ophthalmol.* **1978**, *96*, 664–665. <https://doi.org/10.1001/archophth.1978.03910050360012>.
7. Fung, Y.C. *Biomechanics: Mechanical Properties of Living Tissues*, 2nd ed.; Springer: New York, NY, USA, 1993.

8. Dupps, W.J.; Wilson, S.E. Biomechanics and wound healing in the cornea. *Exp. Eye Res.* **2006**, *83*, 709–720. <https://doi.org/10.1016/j.exer.2006.03.015>.
9. Uchio, E.; Ohno, S.; Kudoh, J.; Aoki, K.; Kisielewicz, L.T. Simulation model of an eyeball based on finite element analysis on a supercomputer. *Br. J. Ophthalmol.* **1999**, *83*, 1106–1111. <https://doi.org/10.1136/bjo.83.10.1106>.
10. Nyquist, G.W. Rheology of the cornea: Experimental techniques and results. *Exp. Eye Res.* **1968**, *7*, 183–188. [https://doi.org/10.1016/s0014-4835\(68\)80064-8](https://doi.org/10.1016/s0014-4835(68)80064-8).
11. Hoeltzel, D.A.; Altman, P.; Buzard, K.; Choe, K.i. Strip Extensimetry for Comparison of the Mechanical Response of Bovine, Rabbit, and Human Corneas. *J. Biomech. Eng.* **1992**, *114*, 202–215. <https://doi.org/10.1115/1.2891373>.
12. Meek, K.M.; Boote, C. The organization of collagen in the corneal stroma. *Exp. Eye Res.* **2004**, *78*, 503–512. <https://doi.org/10.1016/j.exer.2003.07.003>.
13. Wiederholt, M.; Thieme, H.; Stumpff, F. The regulation of trabecular meshwork and ciliary muscle contractility. *Prog. Retin. Eye Res.* **2000**, *19*, 271–295. [https://doi.org/10.1016/s1350-9462\(99\)00015-4](https://doi.org/10.1016/s1350-9462(99)00015-4).
14. Žavbi, J.; Redmon, S.N.; Križaj, D. TRPV4 regulates intraocular pressure through trabecular meshwork contractility and fibrosis. *Channels* **2026**, *20*, 2611702. <https://doi.org/10.1080/19336950.2025.2611702>.
15. Yoshida, Y.; Fujino, Y.; Michihata, N.; Akagi, A.; Koizumi, N.; Okumura, N.; Tanito, M. Effects of Daily Ambient Temperature on Intraocular Pressure: A Time-Series Analysis Using Generalized Additive and Distributed Lag Nonlinear Models. *Investig. Ophthalmol. Vis. Sci.* **2025**, *66*, 76. <https://doi.org/10.1167/iovs.66.15.76>.
16. Johnstone, M.; Xin, C.; Martin, E.; Wang, R. Trabecular Meshwork Movement Controls Distal Valves and Chambers: New Glaucoma Medical and Surgical Targets. *J. Clin. Med.* **2023**, *12*, 6599. <https://doi.org/10.3390/jcm12206599>.
17. Kessel, L.; Johnson, L.; Arvidsson, H.; Larsen, M. The Relationship between Body and Ambient Temperature and Corneal Temperature. *Investig. Ophthalmology Vis. Sci.* **2010**, *51*, 6593. <https://doi.org/10.1167/iovs.10-5659>.
18. Gyftopoulos, E.P.; Beretta, G.P. *Thermodynamics: Foundations and Applications*; Dover: New York, NY, USA, 2005.
19. Cvetković, M.; Peratta, A.; Poljak, D. Exposed To Infrared Radiation Of 1064 Nm Nd:YAG And 2090 Nm Ho:YAG Lasers. In *Environmental Health Risk V*; Brebbia, C.A., Ed.; WIT Press: Southampton, UK, 2009; pp. 221–231. <https://doi.org/10.2495/EHR090221>.
20. Shinoda, K.; Yagura, K.; Matsumoto, S.; Terauchi, G.; Mizota, A.; Miyake, Y. Intraocular Temperature at Different Sites in Eye Measured at the Beginning of Vitreous Surgery. *J. Clin. Med.* **2021**, *10*, 3412. <https://doi.org/10.3390/jcm10153412>.
21. Wang, W.; Qian, X.; Song, H.; Zhang, M.; Liu, Z. Fluid and structure coupling analysis of the interaction between aqueous humor and iris. *Biomed. Eng. Online* **2016**, *15*, 133. <https://doi.org/10.1186/s12938-016-0261-3>.
22. Çengel, Y.; Boles, M.; Kanoğlu, M. *Thermodynamics: And Engineering Approach*; McGraw-Hill: New York, NY, USA, 2019.
23. Canning, C.R.; Greaney, M.J.; Dewynne, J.N.; Fitt, A.D. Fluid flow in the anterior chamber of a human eye. *Math. Med. Biol.* **2002**, *19*, 31–60. <https://doi.org/10.1093/imammb/19.1.31>.
24. Terauchi, R.; Fukai, K.; Ito, K.; Ogawa, S.; Noro, T.; Kato, T.; Kato, K.; Tatemichi, M.; Kabata, Y.; Nakano, T. Association between intraocular pressure and climate parameters. *Sci. Rep.* **2025**, *15*, 41280. <https://doi.org/10.1038/s41598-025-25118-w>.
25. Shiose, Y. Intraocular pressure: New perspectives. *Surv. Ophthalmol.* **1990**, *34*, 413–435. [https://doi.org/10.1016/0039-6257\(90\)90122-c](https://doi.org/10.1016/0039-6257(90)90122-c).
26. Braakman, S.T.; Moore, J.E.; Ethier, C.R.; Overby, D.R. Transport across Schlemm’s canal endothelium and the blood-aqueous barrier. *Exp. Eye Res.* **2016**, *146*, 17–21. <https://doi.org/10.1016/j.exer.2015.11.026>.
27. Shafahi, M.; Vafai, K. Human Eye Response to Thermal Disturbances. *J. Heat Transf.* **2010**, *133*, 011009. <https://doi.org/10.1115/1.4002360>.
28. C., G.K.; Gurung, D.B.; Adhikary, P.R. FEM Approach for Transient Heat Transfer in Human Eye. *Appl. Math.* **2013**, *4*, 30–36. <https://doi.org/10.4236/am.2013.410a2003>.
29. Fabiani, C.; Li Voti, R.; Rusciano, D.; Mutolo, M.G.; Pescosolido, N. Relationship between Corneal Temperature and Intraocular Pressure in Healthy Individuals: A Clinical Thermographic Analysis. *J. Ophthalmol.* **2016**, *2016*, 3076031. <https://doi.org/10.1155/2016/3076031>.
30. Bolivar, G.; Paz, J.; A., M., Cornea and Glaucoma. In *Glaucoma—Basic and Clinical Aspects*; InTech: London, UK, 2013; Chapter 11. <https://doi.org/10.5772/53017>.
31. Mapstone, R. Determinants of corneal temperature. *Br. J. Ophthalmol.* **1968**, *52*, 729–741. <https://doi.org/10.1136/bjo.52.10.729>.
32. Goldmann, H.; Schmidt, T. Über Applanationstonometrie. *Ophthalmologica* **1957**, *134*, 221–242. <https://doi.org/10.1159/000303213>.
33. Morgan, P.B.; Soh, M.P.; Efron, N. Corneal surface temperature decreases with age. *Contact Lens Anterior Eye* **1999**, *22*, 11–13. [https://doi.org/10.1016/s1367-0484\(99\)80025-3](https://doi.org/10.1016/s1367-0484(99)80025-3).
34. Avtar, R.; Srivastava, R. Modelling the flow of aqueous humor in anterior chamber of the eye. *Appl. Math. Comput.* **2006**, *181*, 1336–1348. <https://doi.org/10.1016/j.amc.2006.03.002>.

35. Ehrlich, P. Ueber provocirte Fluorescenzerscheinungen am Auge (Schluss aus No. 3.). *DMW Dtsch. Med. Wochenschr.* **1882**, *8*, 54–55. <https://doi.org/10.1055/s-0029-1196341>.
36. WYATT, H.J. Ocular Pharmacokinetics and Convectional Flow: Evidence from Spatio-Temporal Analysis of Mydriasis. *J. Ocul. Pharmacol. Ther.* **1996**, *12*, 441–459. <https://doi.org/10.1089/jop.1996.12.441>.
37. Galassi, F.; Giambene, B.; Corvi, A.; Falaschi, G. Evaluation of ocular surface temperature and retrobulbar haemodynamics by infrared thermography and colour Doppler imaging in patients with glaucoma. *Br. J. Ophthalmol.* **2007**, *91*, 878–881. <https://doi.org/10.1136/bjo.2007.114397>.
38. Chen, M.J.; Liu, Y.T.; Tsai, C.C.; Chen, Y.C.; Chou, C.K.; Lee, S.M. Relationship Between Central Corneal Thickness, Refractive Error, Corneal Curvature, Anterior Chamber Depth and Axial Length. *J. Chin. Med. Assoc.* **2009**, *72*, 133–137. [https://doi.org/10.1016/s1726-4901\(09\)70038-3](https://doi.org/10.1016/s1726-4901(09)70038-3).
39. Sodi, A.; Giambene, B.; Falaschi, G.; Caputo, R.; Innocenti, B.; Corvi, A.; Menchini, U. Ocular Surface Temperature in Central Retinal Vein Occlusion: Preliminary Data. *Eur. J. Ophthalmol.* **2007**, *17*, 755–759. <https://doi.org/10.1177/112067210701700511>.
40. Matsushashi, K.; Kanamoto, T.; Kurokawa, A. Thermal Model and Countermeasures for Future Smart Glasses. *Sensors* **2020**, *20*, 1446. <https://doi.org/10.3390/s20051446>.
41. Kratz, A.; Yagev, R.; Belkin, A.; Goldberg, M.; Zahavi, A.; Goldberg, I.; Imtirat, A. Comparative Evaluation of Classic Mechanical and Digital Goldmann Applanation Tonometers. *Diagnostics* **2025**, *15*, 1813. <https://doi.org/10.3390/diagnostics15141813>.
42. Munyapa, T.; Mzumara, T.; Ogbonna, G.; Mvula, A. Analysis of Goldman Applanation Tonometry with and without fluorescein among glaucomatous and nonglaucomatous patients attending Mzuzu Central Hospital in Malawi: A cross-sectional study. *Health Sci. Rep.* **2023**, *6*, e1390. <https://doi.org/10.1002/hsr2.1390>.
43. Yasmin, R.; Ahmad, R.; Sultana, N.; Sayed, S.; Ahmad, S.; Zaman, F.; Moniruzzaman. Eye problems among the workers in re-rolling mill exposed to high temperature. *Work* **2013**, *46*, 93–97. <https://doi.org/10.3233/wor-2012-1473>.

Disclaimer/Publisher’s Note: The statements, opinions and data contained in all publications are solely those of the individual author(s) and contributor(s) and not of MDPI and/or the editor(s). MDPI and/or the editor(s) disclaim responsibility for any injury to people or property resulting from any ideas, methods, instructions or products referred to in the content.